ISSN 0252-1075
Research Report No. RR-077

Contribution from

Indian Institute of Tropical Meteorology

UNIVERSAL SPECTRUM FOR INTRASEASONAL VARIABILITY IN TOGA TEMPERATURE TIME SERIES

by

A.M. SELVAM,
M. RADHAMANI,
S. FADNAVIS
and
M.I.R. TINMAKER

PUNE - 411 008
INDIA

AUGUST 1998

CONTENTS

Universal Spectrum for Intraseasonal Variability in TOGA Temperature Time Series

A.M. Selvam, M. Radhamani, S. Fadnavis and M.I.R. Tinmaker

Indian Institute of Tropical Meteorology, Pune 411 008, India

Abstract

Continuous periodogram spectral analyses of 2-day mean upper air TOGA temperature time series at all available standard levels (from 1000 hPa to 250 hPa) for the 92-day period June to August 1988 for the latitude band 50°N to 50°S give the following results. (1) A majority of the spectra follow the universal inverse power law form of the statistical normal distribution with the percentage contribution to total variance representing the percentage probability corresponding to normalised standard deviation equal to (log L / log T_{50}) -1 where L is the period in days and T_{50} the period up to which the cumulative percentage contribution to total variance is equal to 50. (2) Dominant periodicities occur in wavebands, the band-width increasing with period length. (3) There is a continuous smooth rotation of the phase angle with increase in period within a waveband and from one waveband to the next indicating a continuous spiral-like structure for atmospheric flows. Atmospheric low-frequency broadband oscillations of periodicities up to 40 days are seen in all the spectra and is shown to be intrinsic to atmospheric flows. Universal spectrum for atmospheric intraseasonal variability implies predictability of the total pattern of fluctuations. The above results are consistent with a cell dynamical system model for atmospheric flows.

Key Words : Intraseasonal variability, Atmospheric low-frequency variability, Universal spectrum for intraseasonal variability, Chaos, Fractals, Self-organized criticality

1. Introduction

The cooperative existence of fluctuations ranging in size-duration from a few millimeters-seconds (turbulence scale) to thousands of kilometers-years (planetary scale) result in the observed long-range spatiotemporal correlations, namely, fractal geometry to the global cloud cover pattern concomitant with inverse power law form for power spectra of temporal fluctuations documented by Lovejoy and Schertzer (1986) and Tessier et al (1993). Long-range spatiotemporal correlations are ubiquitous to real world dynamical systems and are recently identified as signatures of self-organized criticality (Bak, Tang and Wiesenfeld 1988). The physics of self-organized criticality is not yet identified. It is important to quantify the total pattern of fluctuations in atmospheric flows for predictability studies. Traditional numerical weather prediction models based on Newtonian continuum dynamics are nonlinear and require numerical solutions. Finite precision computer realizations of such nonlinear models are sensitively dependent on initial conditions, now identified as deterministic chaos (Gleick, 1987) resulting in unrealistic solutions. The physics of deterministic chaos is not yet identified. Mary Selvam (1993a) has shown that

round-off error approximately doubles on an average for each step of finite precision numerical iteration. Such round-off error doubling results in unrealistic solutions for numerical weather prediction and climate models which incorporate long-term numerical integration schemes with thousands of such iterations. Realistic modeling of atmospheric flows therefore requires alternative concepts for fluid flows and robust computational techniques which do not require round-off error prone calculus-based long-term numerical integration schemes. In this paper, a recently developed non-deterministic cell dynamical system model for atmospheric flows (Mary Selvam, 1990, 1993a,b, 1996; Mary Selvam et al., 1992; Selvam 1994; Selvam and Radhamani 1994, 1995; Selvam et al., 1994,1995, 1996; Selvam and Joshi 1995) is summarized. The model predicts the observed self-organized criticality, i.e., long-range spatiotemporal correlations as intrinsic to quantum-like mechanics governing atmospheric flow dynamics. Further, the model concepts enable to show that the temporal fluctuations self-organize to form power spectra with universal inverse power law form of the statistical normal distribution. Representative power spectra of upper air TOGA (Tropical Ocean Global Atmosphere) global 1000 hPa to 250 hPa 00 GMT 2-day mean temperature for the 92 day period June to August 1988 are consistent with model predictions. Atmospheric low frequency variability documented by Madden and Julian (1994) is shown to be intrinsic to atmospheric flows powered by the diurnal cycle of solar heating.

A brief introduction to the concept of 'fractals' is first given, followed by the application of cell dynamical system model concepts for prediction of intraseasonal variability of atmospheric flows.

2. Multifractal Structure of Space-Time Fluctuations

Nonlinear dynamical systems in nature such as atmospheric flows exhibit complex spatial patterns, e.g., cloud geometry, that lack a characteristic (single) length scale concomitant with temporal fluctuations that lack a single time scale. The mathematical concept of 'fractals' introduced by Mandelbrot (1977) provides powerful tools for describing and quantifying the universal symmetry of self-similarity (Schroeder 1991) underlying the seemingly irregular complex geometrical shapes and temporal fluctuations.

2.1 Fractal Geometry

Objects in nature are selfsimilar fractals, i.e. the internal small-scale structure resembles the whole object in shape. The fractal dimension D of the such a self-similar object is given as

$$D = \frac{d \ln M}{d \ln R}$$

where M is the mass contained within a distance R from a point in the extended object. A graph of M versus R on logarithmic scale will give a straight line of negative slope D, i.e., the graph exhibits inverse power law form indicating long-range spatial correlations. Constant value for fractal dimension D indicates

logarithmic stretching over the length scale R. Objects in nature exhibit multifractal structure, i.e. the fractal dimension D varies with length scale R range. The region of constant fractal dimension D is associated with scale invariance, namely, the large and small scale structures are related to each other by only the scale ratio independent of the details of nature of growth.

2.2 *Fractals in time*

Spatially extended fractal objects in nature support fluctuations of dynamical processes on all time scales. The power spectra of such broadband fluctuations exhibit inverse power-law of form $1/f^{\alpha}$ where f is the frequency and α the exponent. In general, α decreases with f and approaches 1 for low frequencies. Such spectra, described as $1/f$ or $1/f$-like spectra of temporal fluctuations are ubiquitous to dynamical systems in nature (West and Schlesinger 1989) and has been the subject of extensive investigation during the last 30-40 years. The frequency range over which α is constant therefore exhibits self-similarity or scale invariance in temporal fluctuations, i.e., the fluctuations are fractals in time. The intensity or variance of longer and shorter period fluctuations are mutually related by a scale factor alone independent of the nature of dynamical processes. The fluctuations exhibit long-range temporal correlations. Also, temporal fluctuations exhibit multifractal structure since α varies for different ranges of frequency f. $1/f$ power-law would seem natural and white nose (flat distribution) would be the subject of involved investigation. (West and Shlesinger 1989).

2.3 *Self-organized criticality : space-time fractals*

Till very recently (1988), fractal geometry to the spatial pattern and fractal fluctuations in time of dynamical processes of the same extended dynamical system were treated as two disparate multidisciplinary fields of research (Bak and Chen 1989). The long-range spatiotemporal correlations underlying spatial and temporal power-law behavior of dynamical systems was identified as a unified manifestation of self-organized criticality in 1988 (Bak et al., 1988; Stanley, 1995).

The unifying concept of self-organized criticality underlying fractals, self-similar scaling, broadband frequency spectra and inverse power-law distribution offer new and powerful means of describing certain basic aspects of spatial form and dynamical processes in a dynamical system. The systems in which self-organized criticality is observed range from the physical to the biological to the social. The physical mechanism underlying the observed self-organized criticality is not yet identified. However, the long-range spatial and temporal correlations underlying dynamical evolution implies predictability in space and time of the pattern of evolution of the dynamical system , for example , atmospheric flows.

3. Cell Dynamical System Model for Atmospheric Flows

In summary, the model (Mary Selvam, 1990; Mary Selvam et al., 1992; Mary Selvam, 1993b) is based on Townsend's (Townsend, 1956) concept that large eddies can be visualized as envelopes of enclosed turbulent eddies in turbulent shear flows. The root mean square (r.m.s.) circulation speed W of large eddy of

radius R is the integrated mean of the r.m.s. circulation speeds w_* of enclosed turbulent eddies of radius r and is given as

$$W^2 = \frac{2}{\pi}\frac{r}{R} w_*^2 \quad (1)$$

The eddy length scale ratio r/R is equal to the phase angle $d\theta$ between the eddies. Therefore the phase angle is directly proportional to the variance i.e.,

$$W^2 \propto d\theta \quad (2)$$

Since large eddy is the integrated mean of enclosed turbulent eddies, the energy (kinetic) of large eddies follow normal distribution characteristics according to the Central Limit Theorem in Statistics. The square of the eddy amplitude, namely, the variance, therefore, represents the probability of occurrence. The above result that the additive amplitudes of eddies, when squared, represent the probability density is observed in the subatomic dynamics of quantum systems such as the electron or photon. Atmospheric flows, therefore follow quantum-like mechanical laws.

The model also predicts the logarithmic wind profile relationship for atmospheric flows. The overall envelope of the large eddy traces a logarithmic spiral with the quasiperiodic Penrose tiling pattern for the internal structure. Atmospheric circulation structure therefore consists of a nested continuum of vortex roll circulations (vortices within vortices) with a two-way ordered energy flow between the larger and smaller scales. Such a concept is in agreement with the observed long-range spatiotemporal correlations in atmospheric flow pattern. Conventional power spectrum analysis of such logarithmic spiral circulation structure will reveal a continuum of eddies with progressive increase in phase. The conventional power spectrum plotted as the percentage contribution to total variance versus the logarithm of frequency (period) will now represent the eddy probability density versus the standard deviations of the eddy fluctuations since the logarithm of the eddy wavelength represents the standard deviation, i.e., the root mean square (r.m.s.) value of eddy fluctuations. This follows from the concept of logarithmic wind profile and also that the r.m.s. value of eddy fluctuations at each stage form the mean level for the next stage of eddy growth. The r.m.s. value of eddy fluctuations can be represented in terms of statistical normal distribution as follows. A normalized standard deviation t=0 corresponds to cumulative percentage probability density equal to 50 for the mean value of the distribution. Since the logarithm of the wavelength represents the r.m.s. value of eddy fluctuations, the normalized standard deviation t is defined for the eddy energy spectrum as

$$t = (\log L / \log T_{50}) - 1 \quad (3)$$

where L is the period in days and T_{50} is the period up to which the cumulative percentage contribution to total variance is equal to 50 and t=0. Further, $\log T_{50}$ also represents the mean value for the r.m.s. eddy fluctuations and is consistent with the

concept of the mean level represented by r.m.s. eddy fluctuation. Power spectral analysis will also show that the eddy continuum has embedded dominant wavebands, the bandwidth increasing with period length. The dominant peak periodicities P_n are given as

$$P_n = \tau^n(2+\tau)T \qquad (4)$$

where τ is the golden mean equal to $(1+\sqrt{5})/2 = 1.618$, T is the primary perturbation time period equal to the diurnal (day to night) cycle of solar heating in the present study and n is an integer ranging from negative to positive values including zero. In the following section it is shown that continuous periodogram analyses of 2-day mean upper air mean global TOGA (Tropical Ocean Global Atmosphere) 00 GMT temperature series for the 92 days period June to August 1988 exhibit the signature of model predicted quantum-like mechanics or self-organized criticality i.e., the power spectra follow the universal inverse power law form of the statistical normal distribution.

4. Data and Analysis

Global 1000 hPa to 250 hPa (7 standard pressure levels) 00 GMT 2-day mean upper air temperature data for the 92-day period June to August 1988 was taken from TOGA (Tropical Ocean Global Atmosphere) data sets (Finch,1994) as a representative sample data set. Data was available at 2.5 degree latitude and longitude intervals. Data for latitude belts from 50^oN to 50^oS was considered for the study. The 7 standard pressure levels are 1000, 850, 700, 500, 400, 300, and 250 hPa. The broadband power spectrum of temperature time series can be computed accurately by an elementary, but very powerful method of analysis developed by Jenkinson (1977) which provides a quasi-continuous form of the classical periodogram allowing systematic allocation of the total variance and degrees of freedom of the data series to logarithmically spaced elements of the frequency range (0.5, 0). The periodogram is constructed for a fixed set of 10000(m) periodicities which increase geometrically as $L_m=2\exp(Cm)$ where C=.001 and m=0, 1, 2,....m. The data series Y_t for the N data points was used. The periodogram estimates the set of $A_m\cos(2\pi\nu_m S-\theta_m)$ where A_m, ν_m and θ_m denote respectively the amplitude, frequency and phase angle for the mth periodicity and S is the time, the unit of time being 2 days. The cumulative percentage contribution to total variance was computed starting from the high frequency side of the spectrum. The period T_{50} at which 50% contribution to total variance occurs is taken as reference and the normalized standard deviation t_m values are computed as (Eq.3).

$$t_m = (\log L_m / \log T_{50})-1$$

The cumulative percentage contribution to total variance, the cumulative percentage normalized phase (normalized with respect to the total phase rotation) and the corresponding t values were computed for all grid points where data was available. The mean power (variance) and phase spectra were computed respectively as cumulative percentage contribution to total variance and percentage

of total rotation for each latitude belt from 50°N to 50°S at latitude intervals of 2.5 degrees. Representative spectra are shown separately for northern and southern hemispheres for 1000hPa and 850hPa (Figs 1-4). The statistical normal distribution is also shown in Figs. 1 to 4. It is seen from Figs. 1 to 4 that the mean variance and phase spectra follow each other closely and also the statistical normal distribution. The "goodness of fit" with normal distribution was tested using the standard statistical chi-square test (Spiegel 1961). A majority of the spectra follow normal distribution. Statistical details of data and periodogram estimates as percentages of total number of grid points for each latitude belt are given as follows : (1) Variance spectra follow normal distribution (Fig. 5a). (2) Variance and phase spectra are same (Fig. 5b) . (3) Data series follow normal distribution characteristics (Fig. 5c) (4) Spectra where T_{50} is less than 20 days (Fig. 5d). T_{50} is the period up to which the cumulative percentage contribution to total variance is equal to 50. (5) Spectra which exhibit dominant peak periodicities in wavebands 4-8, 8-12, 12-18, 18-30, 30-50 and 50-90 days (Fig. 6). These wavebands include model predicted (Eq. 4). Dominant periodicities (days) 5.8, 9.5, 15.3, 24.8 and 40.1 for values of n equal to 1,2,3,4 and 5 respectively.

5. Discussion and Conclusion

From Figs. 1-6 it is seen that a majority of spectra of temporal (days) fluctuations of upper air temperature at 00 GMT from 50°N to 50°S, follow the universal and unique inverse power law form of the statistical normal distribution such that the square of the eddy amplitude represents the eddy probability density corresponding to the normalized standard deviation t equal to (log L/log T_{50})-1 where T_{50} is the period up to which the cumulative percentage contribution to total variance is equal to 50. Inverse power law form for power spectra of temporal fluctuations is a signature of self-organized criticality (Bak, Tang and Wiesenfeld, 1988) in the non-linear variability of temperature at all pressure levels in this study. The unique quantification for self-organized criticality in terms of the statistical normal distribution presented in this paper implies predictability of the total pattern of fluctuations in temperature at all pressure levels over a period of time, 92-days in the present study. It may therefore be possible to predict future trends in temperature. Figs. 1-6 also show that the phase spectra closely follow the variance spectra in agreement with model prediction (Eq.2). The continuous smooth rotation of phase angle seen in Figs. 1-4 is consistent with model prediction of spiral-like structure for atmospheric flows. The contribution to temperature fluctuations by shorter periodicities (higher frequencies) is larger in the southern hemisphere as compared to the northern hemisphere(Figs. 5 and 6).

5.1 Applications for prediction

The concept of self-organized criticality, namely, long-range spatial and temporal correlations intrinsic to atmospheric flow patterns forms the basis for statistical prediction models such as the 16-parameter long-range monsoon prediction model of Gowarikar et al (1989).

Observed dominant cycles corresponding to model predicted periodicities (days) 5.8, 9.5, 15.3, 24.8, 40.1 etc. can also be used for prediction purposes.

The effect on intraseasonal variability, of climate change related to man-made greenhouse gas warming, can be qualitatively estimated as follows. Universal spectrum for intraseasonal variability rules out linear secular trends. Energy input into the atmosphere due to greenhouse gas warming will result in intensification of intraseasonal variability which can be seen immediately in the high frequency fluctuations, i.e., intensification of small scale, short period fluctuations.

Detailed application methods for quantitative prediction are under investigation and will be published as a separate paper.

From Fig. 5a it is seen that almost all the 2-day mean data sets follow normal distribution characteristics. A majority of spectra exhibit peak periodicities in wavebands up to 40 days, which corresponds to the well documented (Madden and Julian 1994) atmospheric low frequency variability. Model predicted dominant peak periodicities (Eq.4) are also shown by most of the spectra (Fig. 6).

The important conclusion of the present study is that temperature fluctuations self-organize to form a universal eddy continuum. Such a concept rules out linear secular (days) trends in temperature.

Acknowledgement

The authors are grateful to Dr. A.S.R. Murty for his keen interest and encouragement during the course of the study.

References

Bak, P., Tang, C. and Wiesenfeld, K., Self-organized criticality, *Phys. Rev.* **A 38**, 364-374, 1988.

Bak, P. and Chen, K., The Physics of fractals, *Physica D* **38**, 5-12, 1989.

COADS, *Comprehensive Ocean Atmosphere Data Set* Release 1. NOAA-ERL, Boulder, Co., 1985.

Finch, C.J. TOGA CD-ROM User's Guide, JPL, California Institute of Technology, California, USA., 1994.

Gowariker, V., Thapliyal, V., Sarker, R.P., Mandal, G.S. and D.R. Sikka, Parametric and power regression models : New approach to long range forecasting of monsoon rainfall in India. *Mausam,* **40**, 2, 115-122, 1989.

Gleick, J., Chaos : Making a New Science, Viking, New York, 1987.

Jenkinson, A.F., *A powerful elementary method of spectral analysis for use with monthly, seasonal or annual meteorological time series.* (U.K. Meteorol. Office) Met. O 13 Branch Memorandum No. 57, 1-23, 1977.

Lovejoy, S., and Schertzer, D., Scale invariance, symmetries, fractals and stochastic simulations of atmospheric phenomena, *Bull.Amer.Meteorol.Soc.*, **67**, 21-32, 1986.

Madden, R.A. and Julian, P.R., Observations of the 40-50 day tropical oscillation - a review, *Mon.Wea.Rev.*, **122**, 814-837, 1994.

Mandelbrot, B.B. *Fractals : Form, Chance and Dimension,* W.H. Freeman, San Francisco, 365 pp, 1977.

Mary Selvam, A., Deterministic chaos, fractals and quantumlike mechanics in atmospheric flows, *Can.J.Phys.*, **68**, 831-841, 1990.

Mary Selvam, A., Pethkar, J.S. and Kulkarni, M.K., Signatures of a universal spectrum for atmospheric interannual variability in rainfall time series over the Indian region, *Int'l.J.Climatol.*, **12**, 137-152, 1992.

Mary Selvam, A., Universal quantification for deterministic chaos in dynamical systems, *Appl.Math.Modelling* **17**, 642-649, 1993a.

Mary Selvam, A., A universal spectrum for atmospheric interannual variability of monsoon rainfall over India, *Adv.Atmos.Sci.*, **10(2)**, 221-226, 1993b.

Mary Selvam, A., Quasicrystalline pattern formation in fluid substrates and phyllotaxis. In *Symmetry in Plants,* Barabe, D., and Jean, R.V. (Eds). No. 4, World Scientific Series in Mathematical Biology and Medicine, World Scientific, Singapore, 1996 (in press).

Schroeder, M. *Fractals, chaos and power laws.* W.H. Freeman, San Francisco, 417 pp, 1991.

Selvam, A.M., and Radhamani, M., Signatures of a universal spectrum for nonlinear variability in daily columnar total ozone content, *Adv.Atmos.Sci.* **11(3)**, 335-342, 1994.

Selvam, A.M., Joshi, R.R., and Vijayakumar, R., Self-organized criticality in COAD temperature time series : implications for climate prediction. *Proc. Air and Waste Management Association,* Int'l. Speciality Conf., Global Climate Change, April 5-8, 1994, Phoenix, Arizona, Air and Waste Management Association, Pittsburgh, USA, 196-205, 1994.

Selvam, A.M. The physics of deterministic chaos : implications for global climate model predictions, *Proc. Air and Waste Management Association,* Int'l. Speciality Conf., Global Climate Change, April 5-8, 1994, Phoenix, Arizona, Air and Waste Management Association, Pittsburgh, USA, 412-417, 1994.

Selvam, A.M., and Joshi, R.R., Universal spectrum for interannual variability in COADS global air and sea-surface temperatures, *Int'l.J.Climatol.* **15**, 613-623, 1995.

Selvam, A.M., Pethkar, J.S., and Kulkarni, M.K., Some unique characteristics of atmospheric interannual variability in rainfall time series over India and the United Kingdom, *Adv.Atmos.Sci.* **12(3),** 377-385,1995 .

Selvam, A.M. and Radhamani, M., Universal spectrum for short period (days) variability in atmospheric total ozone, *Mausam* **46(3),** 297-303, 1995.

Selvam, A.M., Pethkar, J.S., Kulkarni, M.K., and Vijayakumar, R., Signatures of a universal spectrum for atmospheric interannual variability in COADS surface pressure time series, *Int'l. J. Climatol.,* **16**, 393-404, 1996.

Spiegel, M.R., *Statistics.* McGraw-Hill Book Co., NY, 359 pp.1961

Stanley, H.E., Power laws and universality, *Nature* **378**, 554,1995.

Tessier, Y., Lovejoy, S., and Schertzer, D., Universal multifractals: theory and observations for rain and clouds, *J.Appl.Meteor.*, **32(2)**, 223-250, 1993.

Townsend, A.A., *The structure of turbulent shear flow*, Cambridge University Press, Cambridge, 1956.

West, B.J. Physiology in fractal dimensions, *Annals of Biomdedical Engineering,* **18**, 135-149.

Legend

Figure 1 : 1000 hPa mean power (variance) and phase spectra for the northern hemisphere.
Figure 2 : Same as Fig. 1 for southern hemisphere.
Figure 3 : 850 hPa mean power (variance) and phase spectra for the northern hemisphere.
Figure 4 : Same as Fig.3 for southern hemisphere.
Figure 5 : Continuous periodogram estimates : Latitudinal means
Figure 6 : Periodogram estimates of dominant wavebands : Latitudinal means

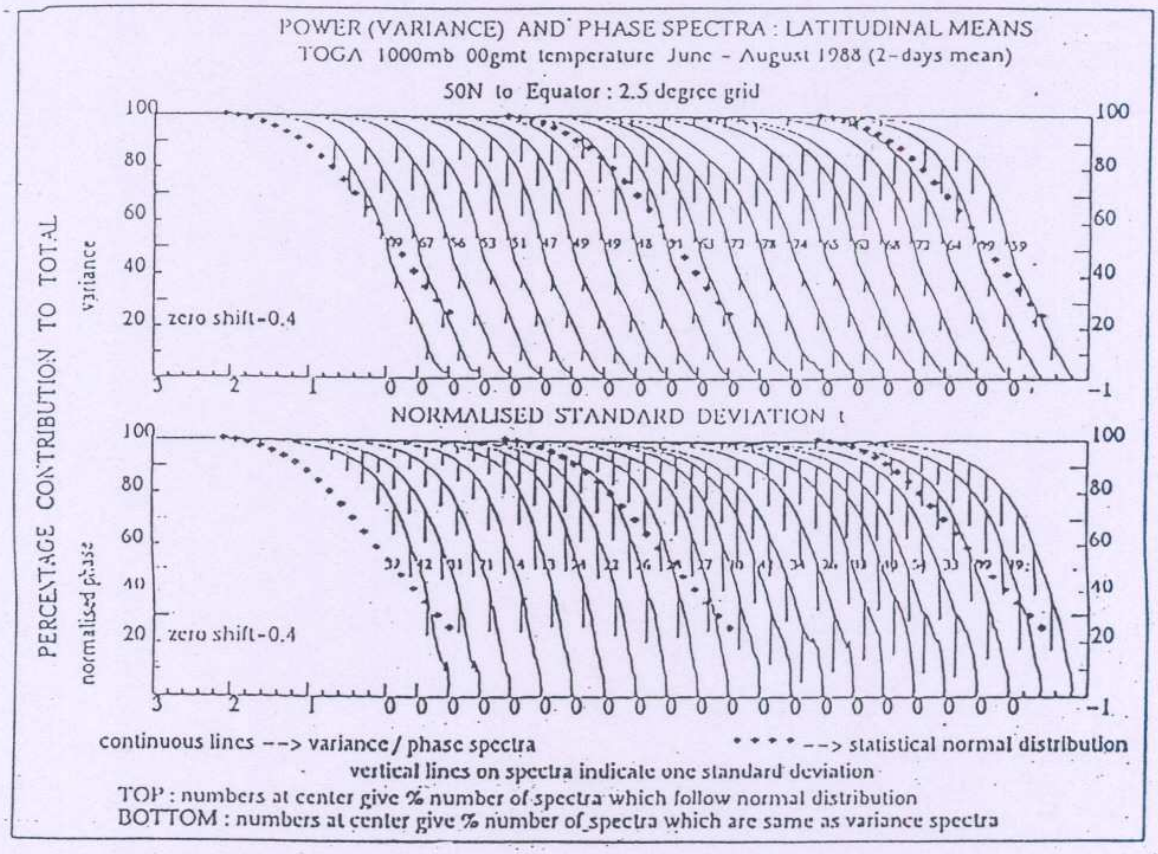

Figure 1 : 1000 mb mean power (variance) and phase spectra for the northern hemisphere.

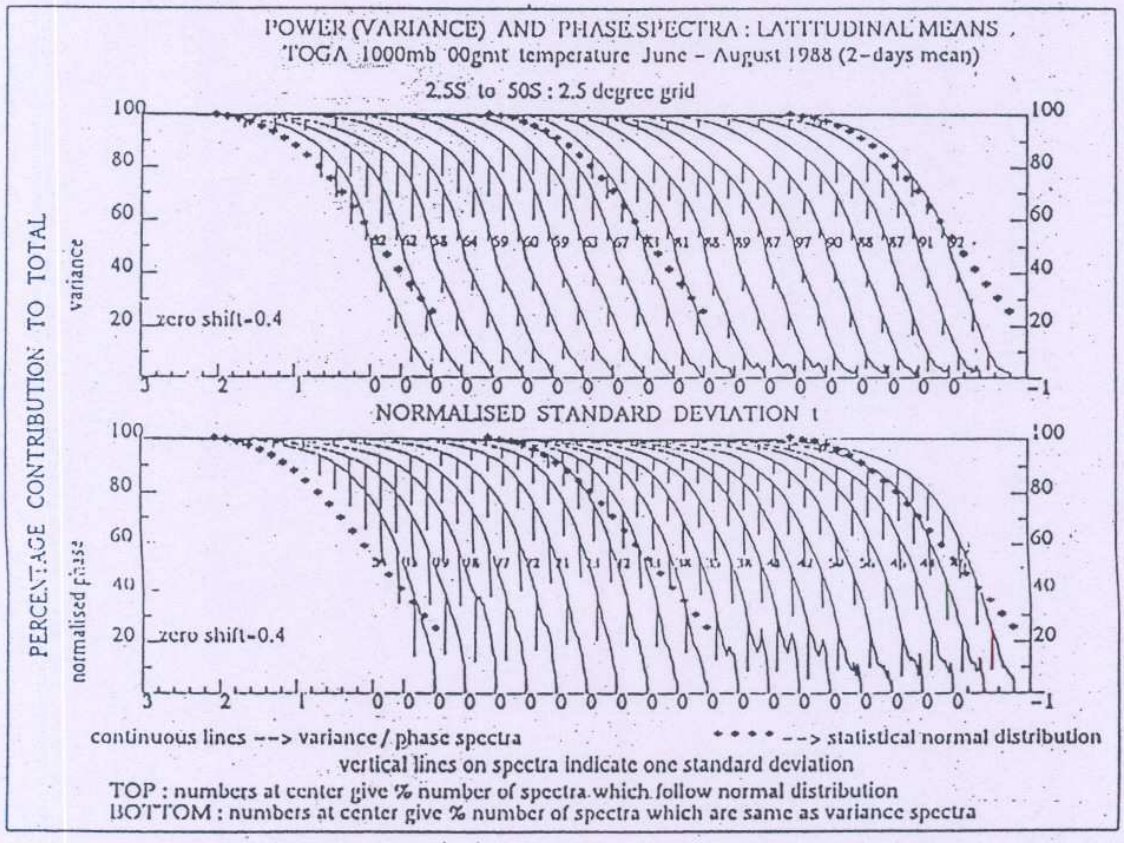

Figure 2 : Same as Fig. 1 for southern hemisphere.

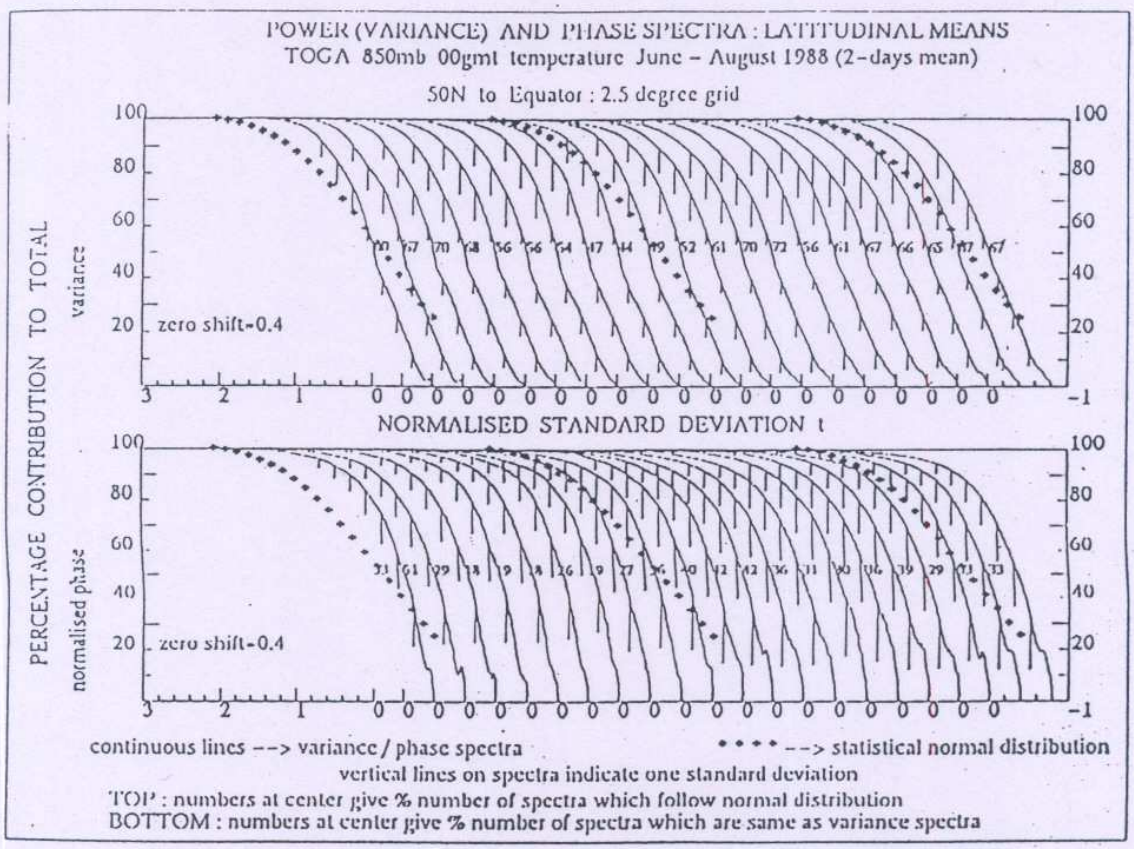

Figure 3 : 850 mb mean power (variance) and phase spectra for the northern hemisphere.

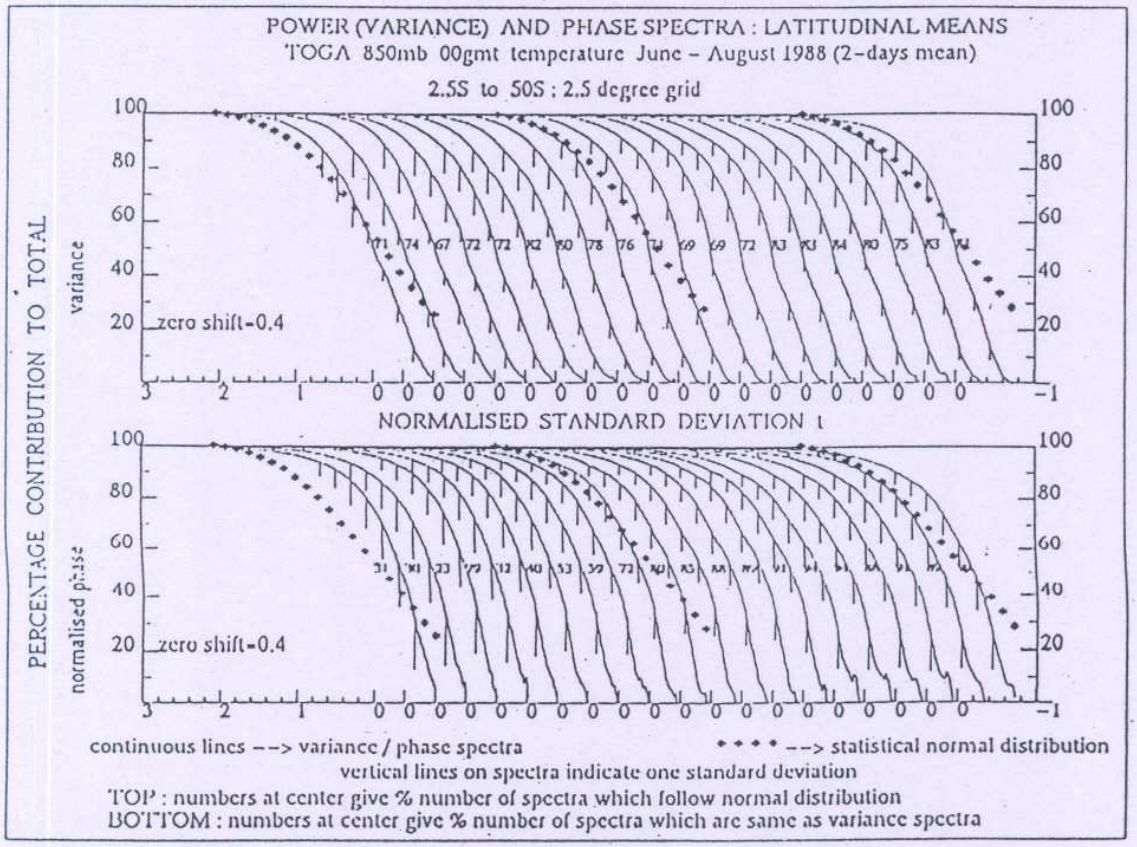

Figure 4 : Same as Fig. 3 for southern hemisphere.

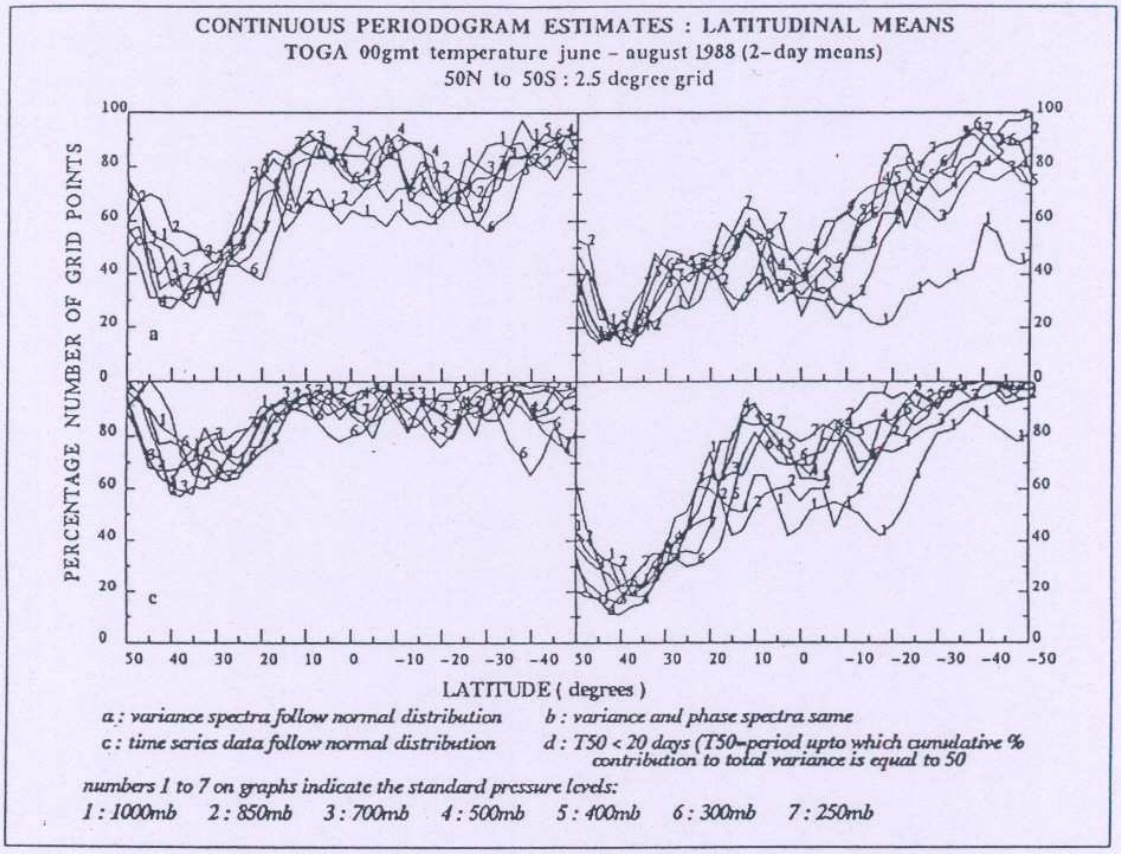

Figure 5 : Continuous periodogram estimates : Latitudinal means.

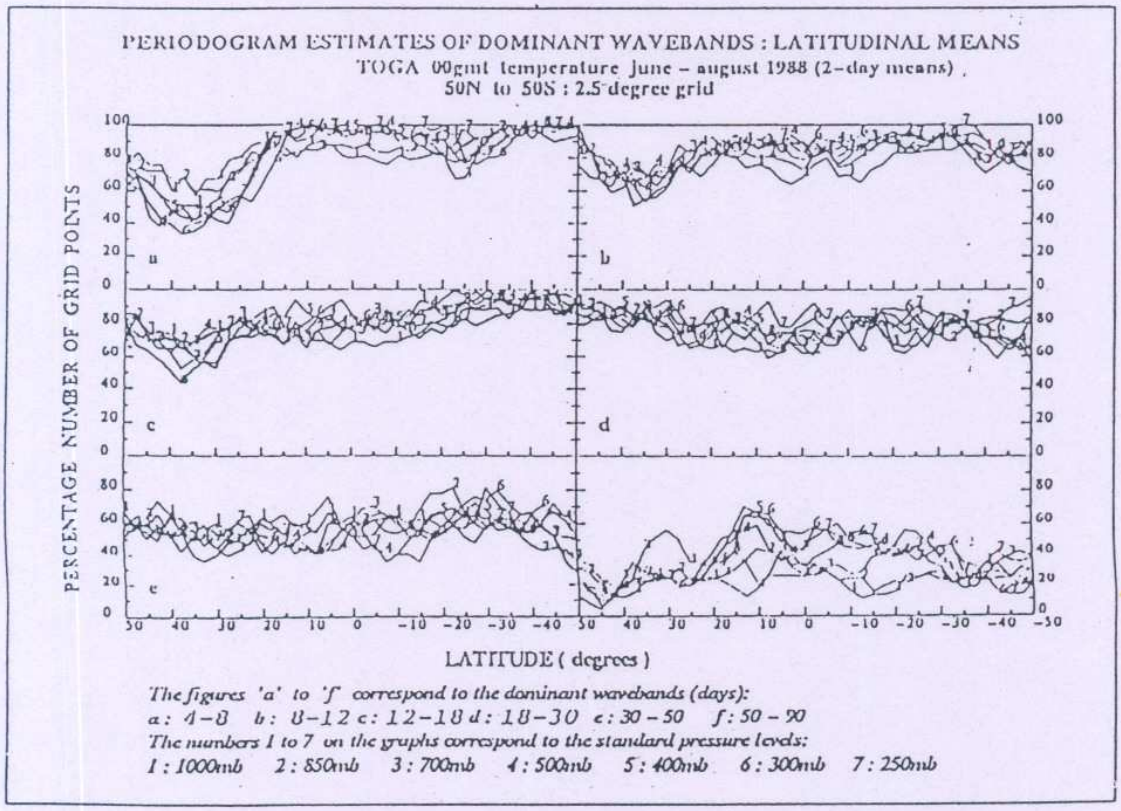

Figure 6 : Periodogram estimates of dominant wavebands : Latitudinal means.